Systems/Circuits

Hippocampal sharp-wave ripples decrease during physical actions including consummatory behavior in immobile rodents

Tomomi Sakairi[1,2]*, Masanori Kawabata[1]*, Alain Rios[1], Yutaka Sakai[2], and Yoshikazu Isomura[1,2]

[1]*Department of Physiology and Cell Biology, Graduate School of Medical and Dental Sciences, Institute of Science Tokyo, Tokyo 113-8519, Japan;*

[2]*Brain Science Institute, Tamagawa University, Tokyo 194-8610, Japan.*

*T.S. and M.K. contributed equally to this work.

Correspondence should be addressed to: Yoshikazu Isomura, PhD, professor
Department of Physiology and Cell Biology, Institute of Science Tokyo
1-5-45 Yushima, Bunkyo-ku, Tokyo 113-8519, Japan
e-mail: isomura.phy2@tmd.ac.jp

Manuscript: 32 pages (Abstract 248 words, Introduction 650 words, and Discussion 1,433 words) **Figures** 6, **Tables** 0, **Multimedia** 0, **3D models** 0.

Conflict of interest: The authors declare no competing financial interests.

Acknowledgments:
This work was supported by Grants-in-Aid for Scientific Research (B) (JP19H03342 and JP23H02589 to Y.I.), for Scientific Research on Innovative Areas (JP20H05053 to Y.I.), for Transformative Research Areas (A) (JP21H05242 to Y.I.), and for Challenging Research (Exploratory) (JP24K21999 to Y.I.) from MEXT and JSPS; by Brain/MINDS (JP19dm0207089 to Y.I.) from AMED; by CREST (JPMJCR1751 to Y.I.) and SPRING (JPMJSP2120 to T.S.) from JST; by the Takeda Science Foundation (Y.I.); and by Center for Brain Integration Research, Institute of Science Tokyo. We appreciate all (former) members of Isomura laboratory, especially Drs. Hidenori Aizawa, Akiko Saiki-Ishikawa, Toshikazu Samura, since this study was inspired by their earlier preliminary observations (Samura T et al. *Neuroscience 2016*, Yokohama, Japan).

Abstract (248/250 words)

Hippocampal sharp-wave ripples (SWRs) are intermittent, fast synchronous oscillations that play a pivotal role in memory formation. It is well known that SWRs occur during "consummatory behaviors", e.g., eating or drinking a reward for correct action. However, most of typical behavioral experiments using freely-moving rodents have not rigorously distinguished eating/drinking itself (regardless of whether it means consummation or consumption) from stopping locomotion (immobility). In this study, therefore, we examined the occurrence of SWRs during a reward-seeking action and subsequent consummatory reward licking in constantly immobile rats under head fixation and body restriction. The immobile rats performed a pedal hold-release action that was rewarded with water every other time for their correct action (false and true consummation). Unexpectedly, the SWRs remarkably decreased during reward licking as well as pedal release action. Unlearned rats also showed a similar SWR decrease during water licking. On the other hand, the SWRs increased gradually during pedal hold period, which was enhanced by reward expectation. A cluster of hippocampal neurons responded to Cue/pedal release and reward as known previously. Some other clusters exhibited spike activity changes similar to the SWR occurrence, i.e., decreasing during the pedal release action and reward licking, and enhanced by reward expectation during pedal hold period. These task event-responsive neurons and SWR-like neurons displayed stronger spiking synchrony with the SWRs than task-unrelated neurons. These findings suggest that the hippocampus generates the SWRs, which may associate action with outcome, in animal's "relative immobility" (action pauses) rather than specific consummation or consumption.

Keywords

Rat, Hippocampus, Sharp-wave ripple, Reward licking, Consummatory behavior, Immobility

Abbreviated title (47/50 letters)

A behavioral determinant of hippocampal ripples

Significance Statement (105/120 words)

To clarify the nature of sharp-wave ripples (SWRs) in the hippocampus, we analyzed the SWRs occurring during operant task performance by immobile rats under head-fixation and body restriction. First, we found the SWRs decreased when they licked and drank water,

which conflicts with the theory that the SWRs occur in consummatory behavior. Second, hippocampal neurons showed different task-related activities, particularly those that resemble the SWR occurrence and those that conveyed specific signals on task events. Third, these task-related neurons displayed strong synchronous discharges during the SWRs in task-engaged periods. These findings may explain the neuronal mechanism underlying the association between an action and its outcome.

Introduction (650/650 words)

Human and animal behaviors can be explained psychologically through *appetitive* (*preparatory*) behavior which seeks appetitive, sexual, or sleep desire, and *consummatory* behavior which finally satisfies the desire (Craig, 1918; Woodworth, 1918; Konorski, 1967; Buzsáki, 2015). For example, when we are thirsty, filling a glass of water from the faucet is a preparatory behavior, while drinking the water is a consummatory behavior (NB, it originally means "consummation" in psychology and ethology, but it is also used as "consumption"). The hippocampus, which is responsible for episodic memory formation, also plays a role in operant action-outcome learning in rodents (Corbit and Balleine, 2000) consisting of preparatory and consummatory behaviors (Osborne and Dodek, 1986; Flaherty et al., 1998; Jurado-Parras et al., 2013). In fact, when rats operantly learn to release a pedal (preparatory behavior) in order to drink water as a reward (consummatory behavior), hippocampal neurons become responsive for those reward-seeking and reward-receiving phases (Soma et al., 2023).

In the hippocampus, high-frequency (100–250 Hz) synchronous oscillation called "ripple" intermittently occurs, accompanied by a brief (40–100 ms) "sharp wave" in local field potentials (sharp-wave ripple, SWR; Buzsáki et al., 1983, 1992; Buzsáki, 1986). Hippocampal pyramidal cells and interneurons discharge synchronously at different phases of the SWR oscillation (Ylinen et al., 1995; Klausberger et al., 2003). The SWRs originate from the hippocampal CA3 area, spread throughout the CA1 area bilaterally (Csicsvari et al., 2000), and propagate into entorhinal and neocortical areas (Chrobak and Buzsáki, 1996), where they are associated with cortical activity (Sirota et al., 2003; Isomura et al., 2006). It is well known that the SWRs occur during consummatory behaviors such as eating and drinking (Buzsáki et al., 1983; Buzsáki, 1986, 2015), in addition to immobility (standstill) and slow-wave sleep that can be regarded as consummatory behaviors in the broad sense (Vanderwolf, 1969; Hartse et al., 1979; Suzuki and Smith, 1985; Buzsáki et al., 1983, 1992; Buzsáki, 1986; O'Neill et al., 2006; Vöröslakos et al., 2023: for review, see Buzsáki 2015; Buzsáki and Tingley, 2023). In contrast, continuous theta (4–12 Hz) oscillations appear instead of the SWRs during whole-body movement (e.g., running) and paradoxical sleep (Vanderwolf 1969; Buzsáki et al., 1983; Buzsáki and Moser, 2013). If animals freely explore space, a set of hippocampal pyramidal cells are activated sequentially along their receptive places during theta oscillations (place cells). Right after they stop running, the place cells are instantly reactivated in the reverse order during the SWRs (replay; Foster and Wilson,

2006; Diba and Buzsaki, 2007). Importantly, the occurrence of SWRs and replays is facilitated by the presence of reward (food/water) at the end of spatial exploration (Singer and Frank, 2009; Ambrose et al., 2016; Sasaki et al., 2018; Sosa and Giocomo, 2021). These observations support the idea that running for exploration is a preparatory behavior for seeking reward, whereas stopping at the reward leads to a consummatory behavior during which the SWRs occur in the hippocampus in dependence on the availability of reward (either expected or acquired).

However, most of behavioral experiments using freely-moving animals have not rigorously distinguished between the immobility (stopping) and reward intake (eating/drinking), even though this is necessary to determine whether the reward expectation or acquisition facilitates the SWR occurrence. In this study, therefore, we investigated how reward expectation and acquisition separately affect the SWR occurrence during preparatory and consummatory behaviors in immobile rats under a head-fixed condition. The head-fixation constantly avoids their whole-body movement and allows for more precise analyses of their behavioral events (pedal release, licking, etc.) than freely-moving conditions. We recorded the SWRs and neuronal spike activity in the hippocampal CA1 area, while the rats performed an operant pedal release task (Soma et al., 2017, 2019, 2023) requiring a rewarded and unrewarded action alternately (Isomura et al., 2013; Yoshizawa et al., 2023). Contrary to the accepted theory, we found that the SWRs and some neuron activity decreased during consummatory reward-intaking action in the immobile rats.

Materials and Methods

Animals.

All experiments were approved by the Animal Research Ethics Committee of Tamagawa University (H28-32, H30-32) and the Animal Care and Use Committee of Tokyo Medical and Dental University (currently, Institute of Science Tokyo; A2019-274, A2021-041, A2023-116), and were performed in accordance with the Fundamental Guidelines for Proper Conduct of Animal Experiment and Related Activities in Academic Research Institutions (Ministry of Education, Culture, Sports, Science, and Technology of Japan (MEXT)) and the Guidelines for Animal Experimentation in Neuroscience (Japan Neuroscience Society). All surgical

procedures were performed under appropriate isoflurane or other anesthesia (see below), and all efforts were made to minimize suffering. Our procedures for animal experiments are described in our previous studies (Isomura et al., 2013; Kimura et al., 2012; 2017; Saiki et al. 2018; Soma et al., 2017, 2019, 2023; Rios et al., 2019, 2023).

Adult Long-Evans rats (Institute for Animal Reproduction; *N* = 9, 159–312 g, male and female) were kept in their home cage under an inverted light schedule (lights off at 9:00 a.m.; lights on at 9:00 p.m.). They were briefly handled (10 min, twice) in advance to adapt to the experimenter and experimental environment.

Surgery.

For head-plate implantation, the rats were anesthetized with isoflurane gas (4.5% for induction and 2.0–2.5% for maintenance, Pfizer) using an inhalation anesthesia apparatus (Univentor 400 anesthesia unit, Univentor) and were placed on a stereotaxic frame (SR-10R-HT, Narishige). Lidocaine jelly (AstraZeneca) was administered around the surgical incisions for local anesthesia. During anesthesia, rectal temperature was maintained at 37 °C using an animal warmer (BWT-100, Bio Research Center). The head-plate (CFR-1, Narishige) was attached to the skull with small stainless anchor screws (M1, 2 mm in length) and dental resin cement (Super-Bond C&B, Sun Medical; Panavia F2.0, Kuraray Medical; Unifast II, GC Corporation). The reference and ground electrodes (Teflon-coated silver wires, A-M Systems; 125 µm in diameter) were implanted on the dura matter above the cerebellum. The skull surface was covered with silicone sealant (DentSilicone-V, Shofu). Analgesics and antibiotics were applied postoperatively, as required (meloxicam, 1 mg/kg *s.c.*, Boehringer Ingelheim; gentamicin ointment, 0.1% *ad us.ext.*, MSD).

After full recovery from this primary surgery (≥5 days later), the rats had *ad libitum* access to water during the weekends, but they obtained water only when they performed the task correctly during the rest of the week. When necessary, agar blocks containing 15 ml water were given to the rats in their home cage to maintain them at >80% of original body weight (Soma et al., 2017, 2019, 2023; Rios et al., 2019, 2023).

Behavioral task.

In our preliminary experiments on natural drinking (see **Fig. 1**), two naïve (unlearned) rats were held immobile with the head fixed to the stereotaxic frame and with the body covered with a stainless-steel cylinder (6 cm in diameter), using the task control system for head-

fixed rodents (TaskForcer; O'HARA & Co., Ltd). They were able to change their posture in place, and soon relaxed in this situation (Kimura et al., 2012). A spout was placed in front of their mouth to dispense a drop of sweet water (0.1% saccharine, 5 µl/drop) from a micropump. Saccharin is not metabolized in the rat body and has negligible effect on blood glucose levels. Therefore, we need not consider the interaction between the SWRs and glucose metabolism (Tingley et al. 2021). Their licking movement with the tongue was monitored by detecting the strain of spout (KFG-2N strain gage and DPM-911B amplifier, Kyowa), which was confirmed by an infrared video camera. The rats passively received two drops of water (10 µl at 150 ms interval) that were delivered from the spout repeatedly every 10–20 s (0.1 s step at random; about 100 times in total) without any prior cues; hence, it was neither classical nor operant conditioning. We recorded hippocampal activity electrophysiologically (see below) during their passive drinking performance from the two rats (*n* = 6 and 5 sessions).

In main experiments on behavioral consummation (see **Fig. 2*A*,*B***), we have established "False-True Consummation (FTC)" task (controlled by the TaskForcer system) in which immobile rats operantly learned to hold and release a pedal with their forelimb (preparatory action) to obtain water as a reward by licking (consummatory action). It was a modified version of our pedal release task for head-fixed rats (Soma et al., 2017, 2019, 2023; Rios et al., 2019, 2023). In this task, the head-fixed rats (*N* = 7 rats; *n* = 59 sessions) spontaneously started each trial by holding down left and right pedals with the corresponding forelimbs for 1–2 s (0.1 s step at random). The position of each pedal was continuously monitored by an angle encoder (hold position: lower 0–20% of full pedal range). After completing the pedal hold time, they had to release the left pedal quickly (within 0.9 s) in response to the presentation of Go cue (10 kHz pure tone for 0.1 s) for the reward, while keeping the right pedal held (0.9 s). The reaction time was defined as the time from the onset of Go cue until the pedal release just started within the hold position.

If they were judged to react correctly, a Correct cue (8 kHz pure tone for 0.3 s) was presented to them 0.1–0.7 s (0.1 s step) after the correct judgement, and two drops of reward water (0.1% saccharine, 10 µl) were ready to be delivered from the spout another 0.3–1.3 s (0.1 s step) after the Correct cue presentation. However, actual reward was given every other trial, i.e., alternating between reward and no-reward trials (reward alternation: Isomura et al., 2013; Yoshizawa et al., 2023). They could confirm that the action was correct by the Correct cue presentation regardless of whether or not rewarded. Such reward

alternation allows rats to easily and naturally predict rewarded or unrewarded for the correct action (Tyler et al., 1953). In this study, we considered a pair of no-reward and subsequent reward trials as "false consummation" and "true consummation" trials for comparison (as described in **Results** and **Fig. 2*B***). If the rats moved the pedals incorrectly, an Error cue (3 kHz square wave tone for 0.3 s) was presented to them immediately, and they were required to retry the same false or true trial (correction trial). If they failed to react to the Go cue (omission), they also retried the correction trial. We analyzed only correct test trials without errors following the previous trials to ensure their reward expectation. They proceeded to the next trial in a self-paced manner after an intertrial interval (ITI; for 1 s). The rats typically learned this operant task in a month (2–3 h training a day) and reached the analysis criteria with ≥30 correct trials a session (42–566 trials/session).

Electrophysiology.

Once the rats recovered from the primary surgery (2 rats for the preliminary experiments) or completed task learning (7 rats for the main experiments), they underwent a secondary surgery under isoflurane anesthesia for later electrophysiological recordings. We made two tiny holes (1.0–1.5 mm in diameter) in the skull and dura matter above the dorsal hippocampi bilaterally (3.8 mm posterior and ±2.0 mm lateral from the bregma). The skull surface and holes were immediately covered with the antibiotic ointment and silicon sealant until the recording experiments.

We performed extracellular multichannel recordings of local field potentials (LFPs) and spike activity of individual neurons in the hippocampal CA1 area while the rats were behaving under the head fixation (11 preliminary sessions from 2 rats; 59 main sessions from 7 rats). Two sets of custom-ordered 64-channel silicon probes (ISO64_4x_tet_lin_A64, NeuroNexus Technologies; 15 tetrodes and 4 tandem electrodes at 150 µm interval on 4 shanks with 50 µm thick) were precisely inserted into the hippocampal CA1 area bilaterally through a supportive layer of agarose gel (2% agarose-HGT, Nacalai Tesque) on the brain surface using fine micromanipulators (SMM-200B, Narishige). The two probes were angled 6–9 degrees towards the medial to avoid mutual interference. The recording depth was determined so as to detect the ripple oscillation of SWRs at the second tetrode from the tip of each probe, which correspond to the stratum pyramidale (s.p.) layer of the hippocampal CA1 area (Csicsvari et al., 2000; Isomura et al., 2006). Hence, the upper and lower (tip) tetrodes were located at the strata oriens (s.o.) and radiatum (s.r.), respectively. The probes

had been inserted at least 1 h before the start of each recording session. In the last recording session, the probes were coated with red fluorescent dye DiI (DiIC18(3), PromoKine) to visualize the tracks later.

The multichannel signals were amplified by two sets of preamplifiers (MPA32I, Multi Channel Systems) and main amplifiers (FA64I, Multi Channel Systems; final gain 2,000, band-pass filter 0.5 Hz–10 kHz), and then digitized and stored at 20 kHz with a 128-channel recorder system (USB-ME128, Multi Channel Systems). The two pedal traces, licking (strain) signal, and task event signals (pedal hold and release, Go cue, Correct cue, reward, error, ITI, etc.) were also digitized and stored simultaneously by the same system.

Histology.

After the final recording experiments, the rats were deeply anesthetized by urethane (2–3 g/kg weight, *i.p.*) and perfused transcardially with cold saline followed by 4% paraformaldehyde in 0.1M phosphate buffer. The whole brain was postfixed, immersed in 30 % sucrose in PB for cryoprotection, and sectioned coronally at 20 µm thick using a cryostat (CryoStar NX50, Epredia). We checked the red fluorescence of probe tracks with DiI and hippocampal CA1 layers counterstained with DAPI (DAPI-Fluoromount-G, SouthernBiotech) under a motorized fluorescence microscope (IX83-DP80, Olympus).

SWR detection.

We detected the SWR events using MATLAB (MathWorks) essentially following standard threshold criteria (Csicsvari et al., 1999, 2000; Isomura et al., 2006; O'Neill et al., 2006). Briefly, the multichannel signals were down-sampled to 1 kHz and filtered at the ripple band (150–250 Hz) *offline*. The filtered signal was squared, smoothed by a Gaussian kernel (σ = 4 ms), taken square root, and z-scored through the entire session for each channel. The SWR candidates were detected by the threshold of 4 standard deviations (SD) from the baseline, and the duration was defined as above the 4 SD. The SWRs with shorter than 30 ms or longer than 200 m were excluded. The peak amplitude and peak time of each SWR event were defined as the negative maximum and its time position of the ripple-band LFP during the event. If the SWRs overlapped among channels, the SWR with the largest amplitude was selected for analysis. Possible artifacts, if contaminated, were eliminated by visual and tailored inspection according to the artifact forms independent of the task information.

Spike isolation and neuron classification.

The multichannel data were also processed to isolate spike events of individual neurons in each tetrode of the silicon probes. Briefly, spike candidates were detected and clustered by the spike-sorting software EToS (Takekawa et al., 2010, 2012). The spike clusters were then manually divided, combined, and discarded by the cluster curation software Klusters and NeuroScope (Hazan et al., 2006) to refine single-neuron clusters based on two criteria: the presence of refractory periods (>2 ms; spike contamination with less than 30% of ongoing spike rate) in their own autocorrelograms and the absence of refractory periods in cross-correlograms with other clusters. We included single-neuron clusters if they exhibited a sufficient number of spike trains during task performance (≥200 trials with total ≥1,000 spikes).

For each neuron (spike cluster), we analyzed its basic spike properties and functional spike activity related to behavioral task performance by the MATLAB as follows. Based on the bimodal distribution of spike duration (from trough to peak; Soma et al., 2023), individual neurons were classified as regular-spiking (RS) neurons (≥0.55 ms; mostly putative pyramidal cells) and fast-spiking (FS) neurons (≤0.5 ms; putative inhibitory interneurons) (see **Fig. 4*A***). The ongoing spike rate was the mean spike rate over the entire time when the neuron was recorded stably throughout the session.

For task-related activity, we analyzed spike trains in relation to two task events (Go cue and reward delivery) separately in the correct trial data for analysis. The spike trains were aligned with the timing (0 s) of these task events and analyzed in 2.0 s time window (−1.0 to +1.0 s from Go cue and −1.0 to +1.0 s from reward delivery). No-reward event (denoted as "pseudo-reward" in the figures) was assumed to occur at the same timing of reward delivery event in each pair of false-true consummation trials for fair comparison in analysis. The task-related activity was defined by the two task relevant indices (TRI*d* and TRI*p*) using *d* and *p* values of Kolmogorov–Smirnov (KS) test (see **Fig. 4*B***; "task-related" if TRI$d \geq 0.1$ AND TRI$p \leq 10^{-5}$ for ≥100 available spikes; see also Kimura et al., 2017; Saiki et al., 2018; Soma et al., 2017, 2019, 2023) for four combinations of the two task events [Go cue and reward/no-reward] with the two trial types [false and true consummation trials]. If one neuron was task-related in any of the four activity patterns, it was referred to as a task-related neuron; otherwise, as non-task-related neuron.

The task-related neurons were further classified into several neuron clusters (Clu.1–4) by the spectral clustering procedure as follows. For each neuron, spike rate patterns were

calculated for −1 to +1 s from the Go cue and for −1 to +3 s from the reward delivery (10 ms bin) in true and false consummation trials. The four patterns were concatenated and z-scored as one 12 s trace. Then, correlation coefficients among all the neurons were calculated to make correlation coefficient matrix. The spectral clustering was performed using the correlation coefficient matrix as the similarity matrix (spectralcluster function in MATLAB, k = 4). The optimal number of clusters was chosen to be the smallest number of clusters for which the value of the smallest eigenvalue of the Laplacian matrix is stationary.

Functional analysis of neural activity.

We used the Phase-Scaling (PS) analysis (Kawabata et al., 2020) to determine which of the two task events (Go cue, pedal release, Correct cue, reward delivery, etc.) with varying interevent intervals was temporally more relevant for neural activity such as the SWRs and neuronal spike activity. This analysis yields the Phase index along trial time normalized by the interevent interval. If the Phase is close to 0, it is more relevant to the first event, and if 1, it is relevant to the second event. We can compute the Phase separately (P− for onset, P+ for offset) for the greatest increasing and decreasing trends in the activity change.

We also evaluated the differential change in SWR occurrence and neuronal activity between false and true consummation trials by the reward modulation index (RMI) defined by the following equation (Isomura et al., 2013; Yoshizawa et al., 2023):

$$\textit{Reward Modulation Index (RMI)} = (SR_t - SR_f) / (SR_t + SR_f)$$

where SR_t and SR_f are the mean spike rates in true and false consummation trials, respectively, in the time window before Go cue (Pre Go cue; 1 s) or after no-reward/reward delivery (Post reward; 2 s). If the RMI is >0, the activity is considered higher in true consummation trials than false, and *vice versa*. The former, RMI (Pre Go cue), would reflect modulation by reward expectation, while the latter, RMI (Post reward), reflect modulation by reward acquisition.

To evaluate the synchrony between the SWRs and spike activity of individual neurons, we made a cross-correlogram (CCG) of the spike sequence of each neuron with the SWR peak at time 0 s. For the CCG analysis, the SWR events without other SWRs nearby (±0.5 s) were collected separately from the task-engaged (on-task) and ITI/resting (off-task) periods. Basically, we analyzed those on-task SWRs in false and true consummation trials together or separately, but no further attempt was made to subdivide the on-task period into trial phases (e.g., pedal hold) due to the insufficiency of SWRs available for analysis.

Spike increase or decrease during the SWRs was first discriminated by comparing the mean spike rate during the SWR time window (±50 ms from the SWR peak) with the overall (±0.5 s), and then judged statistically as a significant change or not by KS test ($d \geq 0.01$ and $p \leq 10^{-5}$). The peak index of spike rate during the SWRs was defined as the difference between two spike rates (true and false; on-task and off-task). The SWR-spike similarity was defined as the correlation coefficient (r) between the SWR rate and spike rate changes aligned with the task event (Go cue or reward).

Statistics.

Data in the text and figures are expressed as mean ± SD or median with quartiles (unless otherwise mentioned) and sample number (n). We used appropriate statistical analyses: Wilcoxon signed-rank test, Wilcoxon rank sum test, Kruskal-Wallis test with post hoc Dunn test, KS test, and chi-square (χ^2) test. The alpha value was set to 0.05 for statistical comparisons, except for using p value as a practical threshold to detect an activity change for the PETH and CCG data.

Results

Hippocampal SWRs during water licking in unlearned immobile rats

It is well established that SWRs appear in the hippocampus during eating and drinking in freely-moving rodents (Buzsáki et al., 1983; Buzsáki, 1986; Buzsáki and Tingley 2023). So first, we conducted a preliminary experiment to check whether the SWRs would also appear when naïve (unlearned) rats drank water in an immobile condition with the head fixation and lower body restriction (**Fig. 1*A***). These immobile rats had never experienced any learning task before, and they naturally licked and drank a drop of water with their tongues delivered from a spout approximately every 10–20 seconds. We recorded SWR activity in the hippocampal CA1 area while monitoring their licking behavior around the delivery of water. Two multichannel silicon probes (64-channels on four shanks) were placed bilaterally along the strata oriens (s.o.), pyramidale (s.p.), and radiatum (s.r.) of dorsal hippocampal CA1 area stereotaxically (**Fig. 1*B***). We clearly observed ripple waves (at putative s.p. layer) and a negative sharp waves (at putative s.r. layer) simultaneously in unfiltered local field potentials (**Fig. 1*C***). We also detected individual lick events using a strain gage sensor

attached to the spout. The SWR and lick events were aligned with the timing of water delivery through all trials of this session (**Fig. 1*D***). The licking was increasing with a slight delay from the water delivery. Contrary to our expectation, the SWR occurrence vanished during licking for the water, and gradually returned to baseline. We failed to observe so prominent theta oscillations during the licking (**Fig. 1*C***). Group data analysis also showed that the SWRs abruptly disappeared in response to the water delivery from the first session, while the licking increased to drink the water (**Fig. 1*E*,*F***; N = 2 rats, n = 11 sessions: SWRs, pre 0.238 ± 0.118 Hz, post 0.076 ± 0.056 Hz, Wilcoxon signed-rank test, $p = 1.28 \times 10^{-4}$, z = 3.83, r = 0.578; Licks, pre 2.07 ± 1.18 Hz, post 5.17 ± 0.88 Hz, $p = 3.34 \times 10^{-3}$, z = −2.93, r = −0.626). Similar results were obtained in different conditions where the water was delivered quicky every few seconds or where the rats had already experienced a learning task sufficiently (data not shown).

Consistent with our preliminary data, it has been briefly reported that the SWRs were reduced during reward licking by head-fixed mice performing a classical conditioning task (see Klee et al., 2021, its Figure Supplement 2B for Figure 5). These observations imply that immobile animals may not necessarily display the SWR generation with the same behavioral characteristics as established by a history of numerous studies on freely-moving animals.

Preparatory and consummatory behaviors in immobile rats

Figure 1 only shows that the SWRs decreased in the case where water was given passively to the immobile rats. The question arises whether such a decrease in SWRs also occurs in immobile rats during licking reward water as a consummatory behavior following an explicit preparatory behavior. Another question is how the expectation of reward affects the SWR occurrence during the preparatory behavior seeking the reward.

To answer these two questions, we trained head-fixed rats to perform an operant learning task (Soma et al., 2017, 2019, 2023) in which they obtained water as a reward (consummatory action) after they correctly operated a pedal with their forelimb (preparatory action) (**Fig. 2*A***). The immobile rats started each trial by holding right and left pedals with both forelimbs for 1–2 s (**Fig. 2*B***; t1). If they correctly released the left pedal quickly (within 0.9 s, t2) and kept holding the other (for 0.9 s) in response to the presentation of Go cue tone (0.1 s at 10 kHz), it was judged to be a correct trial. A Correct cue tone (0.3 s at 8 kHz) was presented to them 0.1–0.7 s (t3) after the correct judgement, and reward

water was ready to be delivered from the spout another 0.3–1.3 s (t4) after the Correct cue presentation. Here, the actual reward was given every other trial, i.e., alternating between reward and no-reward trials (reward alternation: Isomura et al., 2013; Yoshizawa et al., 2023), which made the rats easily and naturally predict rewarded or unrewarded for the action (Tyler et al., 1953). In other words, they must successfully complete a pair of no-reward and reward trials to obtain one reward (**Fig. 2*B***; hereafter, "false" and "true" consummation trials, respectively). According to the psychological definition, it is a (true) consummation to lick and drink the reward water in the true consummation/reward trial. In contrast, we can consider their attempts to lick the spout as a false consummation in the false consummation/no-reward trial. The only difference between them was the presence and absence of actual reward. On the other hand, it is a preparatory action, in definition, to hold and release the pedals to seek the reward in both trials. The external task environment was identical between them; the only difference was the degree of reward expectation that the animals make internally. While the head-fixed rats were performing this "False-True Consummation" (FTC) task, we recorded the SWRs and spike activity in the hippocampal CA1 area bilaterally and monitored their pedal releases by each forelimb and their licks by the tongue. In this way, comparing between the false and true consummation trials, we examined how the reward expectation and acquisition would affect the SWR generation during the preparatory and consummatory actions, respectively.

The head-fixed rats learned to perform the FTC task in a month, and they usually completed several hundreds of pairs of false and true consummation trials in one session. In a typical session, the reaction time to release the pedal from the Go cue presentation was significantly shorter in true consummation trials than in false trials (**Fig. 2*C***), suggesting that the rat internally predicted the presence or absence of upcoming reward when they released the pedal in each trial. Overall, the reaction time was not significantly different between true and false consummation trials due to large individual differences (**Fig. 2*E***; N = 7 rats; n = 59 sessions: False 0.455 ± 0.127 s, True 0.444 ± 0.079 s, Wilcoxon signed-rank test, p = 0.624, z = 0.491, r = 0.064). The rate of "anticipatory licking" prior to the Correct cue presentation was significantly higher in true consummation trials than in false trials in most of the 59 sessions (**Fig. 2*D*,*F***, *left*; False 1.36 ± 1.00 Hz, True 1.93 ± 1.37 Hz, $p = 1.26 \times 10^{-6}$, $z = -4.85$, $r = -0.631$). As expected, the rate of "intake licking" to drink the actual reward from the spout in true consummation trials was remarkably higher than that in false trials (**Fig. 2*D*,*F***, *right*; False 0.84 ± 0.57 Hz, True 4.95 ± 1.04 Hz, $p = 2.39 \times 10^{-11}$, $z = -6.68$, $r = -0.870$).

These results suggest that the reward expectation was reliably reflected into the reaction time (in some sessions) and anticipatory liking rate.

Hippocampal SWRs during preparatory and consummatory actions

We detected the SWRs in the hippocampal CA1 area of the immobile rats that performed the FTC task under head fixation. In a typical session, the SWRs occurred during the pedal hold period, but they decreased rapidly after the Go cue presentation and pedal release (**Fig. 3*A***). The SWR occurrence was much larger in the true consummation trials than the false consummation trials during the pedal hold period. Moreover, the SWR occurrence rapidly ceased again after the Correct cue and delivery of real reward only in the true consummation trials (**Fig. 3*B***). The Correct cue did not affect it in the false consummation trials. Group data showed similar SWR increase during the pedal hold period, which was significantly enhanced in the true consummation trials (**Fig. 3*C***, *left*; n = 59 sessions: False-pre 0.263 ± 0.130 Hz and -post 0.172 ± 0.126 Hz, True-pre 0.433 ± 0.150 Hz and -post 0.230 ± 0.146 Hz: Kruskal Wallis test $p = 8.90 \times 10^{-17}$, $\chi^2 = 77.8$, $\eta^2 = 0.242$; post hoc Dunn test, False-pre vs. False-post $p = 8.52 \times 10^{-4}$, True-pre vs. True-post $p = 1.42 \times 10^{-10}$, False-pre vs. True-pre $p = 3.12 \times 10^{-7}$, False-post vs. True-post $p = 0.0416$, False-pre vs. True-post $p = 0.194$, False-post vs. True-pre $p < 1.00 \times 10^{-100}$). They also showed abrupt disappearance of SWRs after reward delivery (**Fig. 3*C***, *right*; False-pre 0.216 ± 0.148 Hz and -post 0.286 ± 0.168 Hz, True-pre 0.245 ± 0.137 Hz and -post 0.0281 ± 0.0324 Hz: $p = 2.16 \times 10^{-24}$, $\chi^2 = 113$, $\eta^2 = 0.319$; False-pre vs. False-post $p = 0.0307$, True-pre vs. True-post $p < 1.00 \times 10^{-100}$, False-pre vs. True-pre $p = 0.171$, False-post vs. True-post $p < 1.00 \times 10^{-100}$, False-pre vs. True-post $p = 2.32 \times 10^{-13}$, False-post vs. True-pre $p = 1$).

Furthermore, we determined which of the two task events (Go cue or pedal release in **Fig. 3*A***; Correct cue or reward delivery in **Fig. 3*B***) was temporally more related to the SWR decrease in the true consummation trials, by using the Phase-Scaling (PS) analysis (Kawabata et al., 2020). Regarding whether the Go cue or release, the Phase index for offset was bimodally distributed to 0 and 1 (**Fig. 3*D***, *left*), meaning that the SWR decreases were related to either of the two events depending on the individual and the session. As for whether the Correct cue or reward, the Phase for offset was mostly 1 (**Fig. 3*D***, *right*), meaning that the SWRs disappeared at the timing of the reward delivery rather than the Correct cue. Around the reward delivery, however the rats moved their tongue for licking, and might additionally release the pedals to touch the spout or groom the face. Therefore,

we further determined which of the reward delivery and the subsequent first lick and pedal release was most related to the SWR disappearance (**Fig. 3*E***). The analysis clearly indicated that the reward delivery (Phase 0, each) was the most plausible determinant of the SWR disappearance around the consummatory behavior. The SWR disappearance continued for one second after the end of licking bout (**Fig. 3*E***, *left*), and then, the SWRs were gradually recovering toward the next pedal hold-release action (**Fig. 3*E***, *right*). Thus, the SWRs may begin to occur a while after forelimb or tongue movement has been completely stopped. Taken together, the SWRs decreased during the reward acquisition, that is, consummatory licking action in the head-fixed rats.

Hippocampal neuronal activity during preparatory and consummatory actions

We isolated spike activity from hippocampal CA1 neurons (n = 6,216) that were recorded simultaneously with the SWRs during task performance. Based on the spike duration, they were classified into the RS and FS neuron subtypes (**Fig. 4*A***; RS n = 4,794, FS 1,422). As expected, the spike rate of RS (mainly, putative excitatory) neurons was statistically lower than that of FS (putative inhibitory) neurons (RS 1.57 ± 2.56 Hz, FS 3.78 ± 6.92 Hz; Wilcoxon rank sum test $p = 3.53 \times 10^{-23}$, $z = -9.92$, $r = -0.10$). We obtained task-related neurons among them using the TRI*d* and TRI*p* (**Fig. 4*B***; n = 3,213; see **Materials and Methods** for details). These task-related neurons were further classified into four neuron clusters (Clu.1 to 4) using spectral clustering for activity patterns in relation to the FTC task events (**Fig. 4*C***; Clu.1 RS n = 615, FS 85; Clu.2 RS 873, FS 124; Clu.3 RS 691, FS 163; Clu.4 RS 421, FS 241; see **Materials and Methods**).

The spike activity of Clu.1 neurons characteristically decreased after the Go cue (or pedal release) (**Fig. 5*A***; Kruskal Wallis test $p = 2.55 \times 10^{-5}$, $\chi^2 = 24.0$, $\eta^2 = 7.43 \times 10^{-3}$; post hoc Dunn test, True-pre vs. True-post $p = 7.79 \times 10^{-6}$, etc.) and reward delivery ($p = 5.45 \times 10^{-34}$, $\chi^2 = 158$, $\eta^2 = 0.0524$; True-pre vs. -post $p = 2.73 \times 10^{-14}$) in true consummation trials. The activity of Clu.2 decreased only after the reward delivery ($p = 1.38 \times 10^{-99}$, $\chi^2 = 461$, $\eta^2 = 0.103$; True-pre vs. -post $p < 1.00 \times 10^{-300}$). Notably, these activity changes of Clu.1 and 2 neurons, almost half of all task-related neurons, resembled the time-course of SWR occurrence. On the other hand, the Clu.3 neurons showed rapid spike increases in response to the Go cue/release ($p = 4.74 \times 10^{-10}$, $\chi^2 = 46.4$, $\eta^2 = 0.0125$; True-pre vs. -post $p = 2.12 \times 10^{-7}$) and reward delivery ($p = 8.40 \times 10^{-31}$, $\chi^2 = 143$, $\eta^2 = 0.0394$; True-pre vs. -post $p < 1.00 \times 10^{-300}$), while the Clu.4 neurons increased the activity much more slowly after the reward

delivery (p = 1.02 x 10^{-11}, χ^2 = 54.2, η^2 = 0.0190; True-pre vs. -post p = 1.10 x 10^{-9}). Population analysis for each neuron cluster (**Fig. 4*D***) showed that the Clu.1 and Clu.3 neurons changed the spike activity between the Go cue and release. In contrast, the Clu.1–3 neurons at once responded to the reward delivery rather than Correct cue. These temporal profiles of task-related neurons were in good harmony with those of the SWRs (**Fig. 3*D***).

In addition, we evaluated how the activity patterns of these neuron clusters were affected by reward expectation and acquisition in the FTC task, using the RMI (pre Go cue) and RMI (post reward), respectively (see **Materials and Methods**). The RMI (pre Go cue) of Clu.1 and Clu.2 neurons was biased positively (**Fig. 5*B***), meaning their activity was enhanced by reward expectation in the pedal hold period, as expected from the spike rate differences (**Fig. 5*A***; Go cue, False-pre vs. True-pre p = 3.00 x 10^{-3} for Clu.1 and p = 1.20 x 10^{-5} for Clu.2). In contrast, the RMI (post reward) of Clu.1 and Clu.2 neurons was remarkably biased toward the −1 end (**Fig. 5*B***), due to spike rate decrease after reward acquisition (**Fig. 5*A***; Reward, False-post vs. True-post p < 1.00 x 10^{-300} for Clu.1 and p < 1.00 x 10^{-300} for Clu.2). It is worth noting that the distribution of SWRs overlapped with a protrusive part of the Clu.1 and Clu.2 neurons.

Synchrony between SWRs and neuronal activities

Finally, we examined how hippocampal neurons with different functions behaved during the SWRs. As known well, many of all the RS and FS neurons displayed spike increase in synchrony with the SWRs (**Fig. 6*A***). Overall, the percentage of RS neurons showing SWR-coincided spike increases was significantly higher than that of FS neurons (**Fig. 6*B***; 2x4 χ^2 test p = 2.37 x 10^{-75}, χ^2 = 349, V = 0.237). The percentage of task-related neurons with SWR-coincided spike increases was also higher than that of non-task-related neurons (**Fig.6*C***; 2x4 χ^2 test p = 3.49 x 10^{-83}, χ^2 = 385, V = 0.249). The peak distribution of significant spike increases was centered at the peak time of SWRs, while the trough distribution of spike decreases, seen only rarely, was delayed from the peak of the SWRs (**Fig. 6*D***; spike increase −5.00 ± 25.0 ms; decrease 23.0 ± 77.0 ms). In each cycle of ripples, the FS neurons discharged following the RS neurons (**Fig. 6*D***; RS 72.3 ± 44.4°; FS 119 ± 59.7°, Cramér-von Mises test p < 1.00 x 10^{-300}, P = 70.8, η^2 = 0.0387). These results well agreed with previous reports (Ylinen et al., 1995; Csicsvari et al., 1999; Klausberger et al., 2003), confirming that our SWR and spike data were sufficiently reliable for analysis.

Figure 6*E* summarizes spike increases and decreases synchronized with SWRs in the

four clusters of task-related neurons and the non-task-related neurons. The Clu.1 to Clu.3 neurons had more SWR-coincided spike increases compared with the Clu.4 and non-task-related neurons (5x2 χ^2 test p = 2.67 x 10^{-102}, χ^2 = 514, V = 0.203). The actual spike rate during the SWRs correlated negatively with the RMI (post reward) and positively with the SWR-spike similarity (around Go cue and reward in true consummation trials; see **Materials and Methods**) overall for all the neurons [**Fig. 6*F***, *upper*; spike rate during SWR against RMI (post reward) p = 3.21 x 10^{-18}, r = −0.110; against SWR-spike similarity (Go cue, true) p = 1.49 x 10^{-39}, r = 0.166; against SWR-spike similarity (reward, true) p = 4.73 x 10^{-17}, r = 0.106], suggesting functional correlates of the SWR synchrony and task-related activity pattern in hippocampal neurons. The ongoing spike rate also correlated with the RMI and SWR-spike similarities [**Fig. 6*F***, *lower*; ongoing spike rate against RMI (post reward) p = 1.01 x 10^{-106}, r = 0.273; against SWR-spike similarity (Go cue, true) p = 3.53 x 10^{-64}, r = −0.212; against SWR-spike similarity (reward, true) p = 1.23 x 10^{-114}, r = −0.283]. Compared with the overall trends (regression lines), the Clu.1 and Clu.3 neurons always showed higher spike rates, while the non-task-related neurons showed lower (**Fig. 6*F***; sign test). Likewise, cumulative frequency curves revealed that the Clu.1–3 neurons exhibited significantly stronger activation than the Clu.4 and non-task-related neurons (**Fig. 6*G***; *upper*; Kruskal Wallis test p = 5.07 x 10^{-79}, χ^2 = 371, η^2 = 0.0558; post hoc Dunn test, p < 0.05 among all cluster pairs except the Clu.4 and NTR combination), which supports the above observations (**Fig. 6*C,E,F***). On the other hand, the ongoing spike rate, reflecting baseline excitability, was highest in the Clu.3 and Clu.4 neurons and lowest in the Clu.2 and non-task-related neurons (**Fig. 6*G***; *lower*; p = 3.52 x 10^{-76}, χ^2 = 358, η^2 = 0.0539; p < 0.01 among all cluster pairs except the Clu.2 and NTR pair).

Furthermore, the spike rates during the SWRs of the Clu.3 and Clu.4 neurons were slightly higher in true than false consummation trials (**Fig. 6*H***, *left*; Clu.3, one-sample Wilcoxon signed-rank sum test p = 6.84 x 10^{-10}, z = 6.17, r = 0.211; Clu.4 p = 7.82 x 10^{-5}, z = 3.95, r = 0.154), and those of Clu.1–3 neurons were also higher in the on-task than off-task period (**Fig. 6*H***, *right*; Clu.1 p = 6.19 x 10^{-13}, z = 7.20, r = 0.272; Clu.2 p = 7.77 x 10^{-11}, z = 6.51, r = 0.206; Clu.3 p = 1.15 x 10^{-15}, z = 8.01, r = 0.274; NTR p = 1.51 x 10^{-4}, z = 3.79, r = 0.069). Thus, the Clu.1–3 neurons displayed higher spike synchrony with the SWRs than the Clu.4 and non-task-related neurons, especially in the on-task period, and in true consummation trials.

Discussion (1,433/1,500 words)

In freely-moving animals, the hippocampus drives theta oscillations that encode spatial information *online* during exploration, and it drives SWRs that reproduce the information *offline* when they stopped (Foster and Wilson, 2006; Diba and Buzsaki, 2007). At the time, the occurrence of SWRs is facilitated by the presence of reward after the exploratory action (Singer and Frank, 2009; Ambrose et al., 2016; Sosa and Giocomo, 2021). Thus, it is widely accepted that the SWRs occur during consummatory behaviors such as eating and drinking rewards (Buzsáki 2015; Buzsáki and Tingley, 2023) in addition to simple immobility (O'Neill et al., 2006; Vöröslakos et al., 2023). In our immobile rats, however, the SWRs rather disappeared during the consummatory licking action that was triggered by the presentation of reward water in the operant learning task (**Figs. 2,3**). The SWR disappearance due to licking was observed even in immobile rat without any reward learning (**Fig. 1**; cf., already referred to by Klee et al., 2021, supplemental data, for classical conditioning). In contrast, the SWR occurrence increased with reward expectation during the preparatory pedal hold period (**Figs. 2,3**). A group of hippocampal neurons (Clu.3) responded to the Cue/release and reward, while some others (Clu.1,2) showed similar characteristics to the time-course of SWR occurrence as described above (**Figs. 4,5**). These neurons discharged more synchronously with the SWRs than task-unrelated neurons in the on-task period (**Fig. 6**). Taken together, the established theory that the SWRs occur during consummatory behaviors (as either consummation or consumption) does not seem applicable at least to immobile animals drinking under head-fixation and body restriction.

Consummatory behaviors other than eating and drinking, as defined in psychology (Craig, 1918; Woodworth, 1918), would also be informative in understanding the two exclusive modes of hippocampal oscillatory activity (i.e., theta oscillations *online* and SWRs *offline*). One example is animal copulation. Both male ejaculation and female lordosis after the ejaculation are considered as consummatory behaviors that finally satisfy their sexual desire. At this moment, theta oscillations, but not SWRs, are seen in the hippocampus in male (Kurtz and Adler, 1973) and female rats (Kurtz, 1975). Another example is voluntary wheel running for rodents. It can be a consummatory behavior in itself as a natural reward that satisfies the desire (presumably “exercise” for humans) (Brené et al., 2007; Basso and Morrell, 2015; Buhler et al., 2023). During this behavior, theta oscillations, but not SWRs, are seen in the hippocampus (Buhler et al., 2023). Thus, both modes of hippocampal oscillatory activity can participate in consummatory behaviors satisfying desires (appetite,

sexual, sleep, etc.) in the classical psychological definition. In other words, the idea that the hippocampal SWRs occur during consummatory behaviors is difficult to generalize to all kinds of the consummatory behaviors.

So why do the SWRs behave differently in the same consummatory licking action between freely-moving and head-fixed conditions? We would presume that the SWRs are prone to appear during no or relatively less movement, i.e., at a pause before and after physical actions, independent of behavioral consummation. In the freely-moving condition, running involves heavy whole-body movement, whereas stopping to eat or drink would result in relatively less movement. Such "relative immobility" (or action pause) might bring about more SWRs in the hippocampus. Under the head-fixed immobilization, the whole body is kept motionless, and thereby, theta oscillations are hardly driven in the hippocampus. Even though the pedal hold action is part of preparatory behavior, it is relative immobility without limb and tongue movements, thereby allowing the SWR generation in the hippocampus. Then the SWRs are temporarily diminished by the pedal release that reduces the immobility. Once a real reward is delivered, the SWRs disappear owing to further reduction in the immobility by drinking the reward intentionally. In fact, we have recently observed that the SWR occurrence dropped when any part of the whole body (jaw, nose, whiskers, limbs, trunk, tail, etc.) moved physically in similar immobile rats (Rios et al., 2024). Thus, the relative immobility can better explain the difference in the SWR occurrence between the freely-moving and head-fixed conditions.

Upon closer inspection, the SWRs disappeared sharply at the timing of reward delivery itself rather than the anticipatory/intake licking or additional pedal releases (**Fig. 3*D*,*E***). Also, the Correct cue prior to reward did not affect the SWR occurrence (**Fig. 3*D***). Therefore, the intrinsic factor that breaks the SWR occurrence is likely to be *internal* information on the *intended* action rather than downstream actual muscular movements or upstream perceptual/motivational processes. We can speculate that animals might rehearse and review each action through hippocampal SWR activity (preplay, Davidson et al., 2009; Gupta et al., 2010; Dragoi and Tonegawa, 2011; replay, Foster and Wilson, 2006; Diba and Buzsaki, 2007) at action pauses before and after the intended action, as if they think then move, stop then think. Maybe it is a natural and ongoing property of ordinary brain operation, as recently reported the correlation between SWRs and internal thought patterns in human daily life (Iwata et al. 2024). It is, therefore, quite possible that immobile animals also produce such functional SWRs for rehearsal and review of their intended

actions.

Here, we propose a hypothesis to account for the neuronal mechanism of action-outcome association in our experimental condition (**Fig. 6*I***). First, the hippocampal neurons playing a direct role in task performance are the Clu.3 neurons that convey phasic signals on the action and its outcome reward. Our previous study showed that such hippocampal neurons emerge spike activity related to the action and reward in the progress of operant learning (Soma et al. 2023). Unlike the Clu.3 neurons, the Clu.1 and Clu.2 neurons work together with the SWR occurrence during the pedal hold period, depending on the degree of reward expectation. It is possible that the Clu.1 and Clu.2 neurons may participate in the framework for SWR activity by elevating their excitability. If so, once an SWR occurs through the Clu.1 and Clu.2 neurons before the action, the Clu.3 neurons may also become active for *offline* reviewing the previous trial or rehearsing the current trial. Perhaps the SWRs occurring after reward acquisition would have a similar effect on those neurons. The Clu.3 neurons themselves might have grown from action-related neurons and reward-related neurons (Soma et al. 2023) as a result of their associative spiking driven by the SWRs in the course of this operant learning. Thus, our hypothesis explains the process of association between action and outcome.

As shown in freely-moving animals (Singer and Frank, 2009; Ambrose et al., 2016; Sosa and Giocomo, 2021), reward expectation enhances the SWR occurrence as well as Clu.1 and Clu.2 neuron activity during the pedal hold period in our immobile rats. This would be advantageous for effectively increasing opportunities to reinforce the association of action and outcome. Interestingly, we found that reward expectation enhances neuronal activity related to Go cue and push-pull actions in the dopamine reward system of the basal ganglia (Rios et al. 2023). It suggests that the dopamine reward system can affect the Clu.3 neurons rather than the SWRs and Clu.1 and Clu.2 neurons in the hippocampus. The basal ganglia may facilitate the optimization of the action based on its outcome by using the SWR-involved episodic memory system in the hippocampus repetitively during the operant learning.

This study provides evidence that a physical action under whole-body immobility critically determines the ability to generate the SWRs in the hippocampus. Today, head fixation protocols are widely used in many neuroscience experiments using rodents and primates, because they have practical advantages not only for accurate behavioral assessment of limbs, tongue, and whiskers, but also for electrical and optical measurement

and manipulation of neural activity at high spatial and temporal resolution. If such useful head fixation is combined with virtual reality that mimics visual or auditory perception in a freely-moving context, we can causally test cognitive brain functions even in unreal circumstances (e.g., Harvey et al. 2009). Furthermore, the brain status during head and body immobility may be relevant not only to experimental animal behaviors but also to our human daily life. Consistent with our observation, Iwata et al. (2024) have recently reported that the SWRs decrease during meals in the hippocampus of human subjects. Then, for instance, does our hippocampus bear a different mode when drinking water while jogging from while sitting in an airplane seat? Does the hippocampus serve cognitive and memory functions in bedridden patients differently from ambulatory patients? Mobility or immobility would be a basic determinant of brain functions. Our findings will shed new light on the dichotomous mechanisms of hippocampal oscillatory activity for cognition and memory by interpreting the behavioral significance of actions and action pauses in distinct physical situations.

References

Ambrose RE, Pfeiffer BE, Foster DJ (2016) Reverse replay of hippocampal place cells is uniquely modulated by changing reward. Neuron 91:1124-1136. doi: 10.1016/j.neuron.2016.07.047.

Basso JC, Morrell JI (2015) The medial prefrontal cortex and nucleus accumbens mediate the motivation for voluntary wheel running in the rat. Behav Neurosci 129:457-472. doi: 10.1037/bne0000070.

Brené S, Bjørnebekk A, Aberg E, Mathé AA, Olson L, Werme M (2007) Running is rewarding and antidepressive. Physiol Behav 92:136-140. doi: 10.1016/j.physbeh.2007.05.015.

Buhler CM, Basso JC, English DF (2023) Hippocampal sharp wave-ripple dynamics in NREM sleep encode motivation for anticipated physical activity. bioRxiv 2023.03.14.532638. doi: 10.1101/2023.03.14.532638.

Buzsáki G (1986) Hippocampal sharp waves: their origin and significance. Brain Res 398:242-252. doi: 10.1016/0006-8993(86)91483-6.

Buzsáki G (2015) Hippocampal sharp wave-ripple: A cognitive biomarker for episodic memory and planning. Hippocampus 25:1073–1188. doi: 10.1002/hipo.22488.

Buzsáki G, Moser EI (2013) Memory, navigation and theta rhythm in the hippocampal-entorhinal system. Nat Neurosci 16:130-138. doi: 10.1038/nn.3304.

Buzsáki G, Tingley D (2023) Cognition from the body-brain partnership: Exaptation of memory. Annu Rev Neurosci 46:191–210. doi: 10.1146/annurev-neuro-101222-110632.

Buzsáki G, Leung LW, Vanderwolf CH (1983) Cellular bases of hippocampal EEG in the behaving rat. Brain Res 287:139-171. doi: 10.1016/0165-0173(83)90037-1.

Buzsáki G, Horváth Z, Urioste R, Hetke J, Wise K (1992) High-frequency network oscillation in the hippocampus. Science 256:1025-1027. doi: 10.1126/science.1589772.

Chrobak JJ, Buzsáki G (1996) High-frequency oscillations in the output networks of the hippocampal-entorhinal axis of the freely behaving rat. J Neurosci 16:3056-3066. doi: 10.1523/JNEUROSCI.16-09-03056.1996.

Corbit LH, Balleine BW (2000) The role of the hippocampus in instrumental conditioning. J Neurosci 20:4233-4239. doi: 10.1523/JNEUROSCI.20-11-04233.2000.

Craig W (1918) Appetites and aversions as constituents of instincts. Biol Bull 34:91-107.

Csicsvari J, Hirase H, Czurkó A, Mamiya A, Buzsáki G (1999) Fast network oscillations in the hippocampal CA1 region of the behaving rat. J Neurosci 19:RC20. doi:

10.1523/JNEUROSCI.19-16-j0001.1999.

Csicsvari J, Hirase H, Mamiya A, Buzsáki G (2000) Ensemble patterns of hippocampal CA3-CA1 neurons during sharp wave-associated population events. Neuron 28:585-594. doi: 10.1016/s0896-6273(00)00135-5.

Davidson TJ, Kloosterman F, Wilson MA (2009) Hippocampal replay of extended experience. Neuron 63:497-507. doi: 10.1016/j.neuron.2009.07.027.

Diba K, Buzsáki G (2007) Forward and reverse hippocampal place-cell sequences during ripples. Nat Neurosci 10:1241-1242. doi: 10.1038/nn1961.

Dragoi G, Tonegawa S (2011) Preplay of future place cell sequences by hippocampal cellular assemblies. Nature 469:397-401. doi: 10.1038/nature09633.

Flaherty CF, Coppotelli C, Hsu D, Otto T (1998) Excitotoxic lesions of the hippocampus disrupt runway but not consummatory contrast. Behav Brain Res 93:1-9. doi: 10.1016/s0166-4328(97)00138-1.

Foster DJ, Wilson MA (2006) Reverse replay of behavioural sequences in hippocampal place cells during the awake state. Nature 440:680-683. doi: 10.1038/nature04587.

Gupta AS, van der Meer MA, Touretzky DS, Redish AD (2010) Hippocampal replay is not a simple function of experience. Neuron 65:695-705. doi: 10.1016/j.neuron.2010.01.034.

Hartse KM, Eisenhart SF. Bergmann BM, Rechtschaffen A (1979) Ventral hippocampus spikes during sleep, wakefulness, and arousal in the cat. Sleep 1:231-246. doi: 10.1093/sleep/1.3.231.

Harvey CD, Collman F, Dombeck DA, Tank DW. Intracellular dynamics of hippocampal place cells during virtual navigation. Nature 461:941-946. doi: 10.1038/nature08499.

Hazan L, Zugaro M, Buzsáki G (2006) Klusters, NeuroScope, NDManager: a free software suite for neurophysiological data processing and visualization. J Neurosci Methods 155:207-216. doi: 10.1016/j.jneumeth.2006.01.017.

Isomura Y, Sirota A, Ozen S, Montgomery S, Mizuseki K, Henze DA, Buzsáki G (2006) Integration and segregation of activity in entorhinal-hippocampal subregions by neocortical slow oscillations. Neuron 52:871-882. doi: 10.1016/j.neuron.2006.10.023.

Isomura Y, Takekawa T, Harukuni R, Handa T, Aizawa H, Takada M, Fukai T (2013) Reward-modulated motor information in identified striatum neurons. J Neurosci 33:10209-10220. doi: 10.1523/JNEUROSCI.0381-13.2013.

Iwata T, Yanagisawa T, Ikegaya Y, Smallwood J, Fukuma R, Oshino S, Tani N, Khoo HM, Kishima H (2024). Hippocampal sharp-wave ripples correlate with periods of naturally occurring

self-generated thoughts in humans. Nat Commun 15:4078. doi: 10.1038/s41467-024-48367-1.

Jurado-Parras MT, Sánchez-Campusano R, Castellanos NP, del-Pozo F, Gruart A, Delgado-García JM (2013) Differential contribution of hippocampal circuits to appetitive and consummatory behaviors during operant conditioning of behaving mice. J Neurosci 33:2293-2304. doi: 10.1523/JNEUROSCI.1013-12.2013.

Kawabata M, Soma S, Saiki-Ishikawa A, Nonomura S, Yoshida J, Ríos A, Sakai Y, Isomura Y (2020) A spike analysis method for characterizing neurons based on phase locking and scaling to the interval between two behavioral events. J Neurophysiol 124:1923-1941. doi: 10.1152/jn.00200.2020.

Kimura R, Saiki A, Fujiwara-Tsukamoto Y, Ohkubo F, Kitamura K, Matsuzaki M, Sakai Y, Isomura Y (2012) Reinforcing operandum: rapid and reliable learning of skilled forelimb movements by head-fixed rodents. J Neurophysiol 108:1781-1792. doi: 10.1152/jn.00356.2012.

Kimura R, Saiki A, Fujiwara-Tsukamoto Y, Sakai Y, Isomura Y (2017) Large-scale analysis reveals populational contributions of cortical spike rate and synchrony to behavioural functions. J Physiol 595:385-413. doi: 10.1113/JP272794.

Klausberger T, Magill PJ, Márton LF, Roberts JD, Cobden PM, Buzsáki G, Somogyi P (2003) Brain-state- and cell-type-specific firing of hippocampal interneurons in vivo. Nature 421:844-848. doi: 10.1038/nature01374.

Klee JL, Souza BC, Battaglia FP (2021) Learning differentially shapes prefrontal and hippocampal activity during classical conditioning. elife 10:e65456. doi: 10.7554/eLife.65456.

Konorski J (1967) Integrative activity of the brain. Chicago: University of Chicago Press.

Kurtz RG, Adler NT (1973) Electrophysiological correlates of copulatory behavior in the male rat: evidence for a sexual inhibitory process. J Comp Physiol Psychol 84:225-239. doi: 10.1037/h0035265.

Kurtz RG (1975) Hippocampal and cortical activity during sexual behavior in the female rat. J Comp Physiol Psychol 89:158-169. doi: 10.1037/h0076650.

O'Neill J, Senior T, Csicsvari J (2006) Place-selective firing of CA1 pyramidal cells during sharp wave/ripple network patterns in exploratory behavior. Neuron ;49:143-155. doi: 10.1016/j.neuron.2005.10.037.

Osborne B, Dodek AB (1986) Disrupted patterns of consummatory behavior in rats with

fornix transections. Behav Neural Biol 45:212-222. doi: 10.1016/s0163-1047(86)90783-1.

Rios A, Soma S, Yoshida J, Nonomura S, Kawabata M, Sakai Y, Isomura Y (2019) Differential changes in the lateralized activity of identified projection neurons of motor cortex in hemiparkinsonian rats. eNeuro 6:ENEURO.0110-19.2019. doi: 10.1523/ENEURO.0110-19.2019.

Rios A, Nonomura S, Kato S, Yoshida J, Matsushita N, Nambu A, Takada M, Hira R, Kobayashi K, Sakai Y, Kimura M, Isomura Y (2023) Reward expectation enhances action-related activity of nigral dopaminergic and two striatal output pathways. Commun Biol 6:914. doi: 10.1038/s42003-023-05288-x.

Rios A, Usui M, Isomura Y (2024) Modulation of hippocampal sharp-wave ripples by behavioral states and body movements in head-fixed rodents. bioRxiv doi: *****

Saiki A, Sakai Y, Fukabori R, Soma S, Yoshida J, Kawabata M, Yawo H, Kobayashi K, Kimura M, Isomura Y (2018) In vivo spiking dynamics of intra- and extratelencephalic projection neurons in rat motor cortex. Cereb Cortex 28:1024-1038. doi: 10.1093/cercor/bhx012.

Sasaki T, Piatti VC, Hwaun E, Ahmadi S, Lisman JE, Leutgeb S, Leutgeb JK (2018) Dentate network activity is necessary for spatial working memory by supporting CA3 sharp-wave ripple generation and prospective firing of CA3 neurons. Nat Neurosci 21: 258-269. doi: 10.1038/s41593-017-0061-5.

Singer, AC, Frank LM (2009) Rewarded outcomes enhance reactivation of experience in the hippocampus. Neuron 64:910-921. doi: 10.1016/j.neuron.2009.11.016.

Sirota A, Csicsvari J, Buhl D, Buzsáki G (2003) Communication between neocortex and hippocampus during sleep in rodents. Proc Natl Acad Sci USA 100:2065-2069. doi: 10.1073/pnas.0437938100.

Soma S, Saiki A, Yoshida J, Ríos A, Kawabata M, Sakai Y, Isomura Y (2017) Distinct laterality in forelimb-movement representations of rat primary and secondary motor cortical neurons with intratelencephalic and pyramidal tract projections. J Neurosci 37:10904-10916. doi: 10.1523/JNEUROSCI.1188-17.2017.

Soma S, Yoshida J, Kato S, Takahashi Y, Nonomura S, Sugimura YK, Ríos A, Kawabata M, Kobayashi K, Kato F, Sakai Y, Isomura Y (2019) Ipsilateral-dominant control of limb movements in rodent posterior parietal cortex. J Neurosci 39:485-502. doi: 10.1523/JNEUROSCI.1584-18.2018.

Soma S, Ohara S, Nonomura S, Suematsu N, Yoshida J, Pastalkova E, Sakai Y, Tsutsui K-I,

Isomura Y (2023) Rat hippocampal CA1 region represents learning-related action and reward events with shorter latency than the lateral entorhinal cortex. Commun Biol 6:584. doi: 10.1038/s42003-023-04958-0.

Sosa M, Giocomo LM (2021) Navigating for reward. Nat Rev Neurosci. 22:472-487. doi: 10.1038/s41583-021-00479-z.

Suzuki SS, Smith GK (1885) Single-cell activity and synchronous bursting in the rat hippocampus during waking behavior and sleep. Exp Neurol 89:71-89. doi: 10.1016/0014-4886(85)90266-3.

Takekawa T, Isomura Y, Fukai T (2010) Accurate spike sorting for multi-unit recordings. Eur J Neurosci 31:263-272. doi: 10.1111/j.1460-9568.2009.07068.x.

Takekawa T, Isomura Y, Fukai T (2012) Spike sorting of heterogeneous neuron types by multimodality-weighted PCA and explicit robust variational Bayes. Front Neuroinform 6:5. doi: 10.3389/fninf.2012.00005.

Tingley D, McClain K, Kaya E, Carpenter J, Buzsáki G (2021) A metabolic function of the hippocampal sharp wave-ripple. Nature 597:82-86. doi: 10.1038/s41586-021-03811-w.

Tyler DW, Wortz EC, Bitterman ME (1953) The effect of random and alternating partial reinforcement on resistance to extinction in the rat. Am J Psychol 66:57-65.

Vanderwolf CH (1969) Hippocampal electrical activity and voluntary movement in the rat. Electroencephalogr Clin Neurophysiol 26, 407-418. doi: 10.1016/0013-4694(69)90092-3.

Vöröslakos M, Zhang Y, McClain K, Huszár R, Rothstein A, Buzsáki G (2023) ThermoMaze: A behavioral paradigm for readout of immobility-related brain events. bioRxiv 2023.07.25.550518. doi: 10.1101/2023.07.25.550518.

Woodworth R (1918) Dynamic Psychology. New York: Columbia University Press.

Ylinen A, Bragin A, Nádasdy Z, Jandó G, Szabó I, Sik A, Buzsáki G (1995) Sharp wave-associated high-frequency oscillation (200 Hz) in the intact hippocampus: network and intracellular mechanisms. J Neurosci 15:30-46. doi: 10.1523/JNEUROSCI.15-01-00030.1995.

Yoshizawa T, Miyamura Y, Ochi Y, Hira R, Funahashi M, Sakai Y, Cui Y, Isomura Y (2023) Working memory-based and -free reward prediction in a dual dopamine system in the basal ganglia. bioRxiv 2023.03.06.531239. doi: 10.1101/2023.03.06.531239.

Figure legends

Figure 1 Hippocampal sharp-wave ripples (SWRs) disappeared during drinking water in naïve (unlearned) immobile rats.

A, Schematic diagram of electrophysiological recording from bilateral hippocampi of a head-fixed rat licking a drop of water from a spout (10–20 s at random interval). LFP, local field potential.

B, Silicon probe tracks in the hippocampal CA1 area (arrowheads, stained with DiI on probe shanks). s.o., stratum oriens; s.p., s. pyramidale; s.r., s. radiatum.

C, *Left*, Two SWR events prior to water delivery (0 s) in raw local field potential (LFP) traces. *Right*, the SWR traces enlarged from left rectangles (ripple oscillations and sharp waves at s.p. and s.r., respectively). Note no artifact noises caused by liking (vertical symbols).

D, *Top*, Ten consecutive LFP traces with SWRs (red arrows) detected within ±2.5 s from water delivery (0 s), filtered at ripple (*each upper*, 150–250 Hz) and sharp wave (*lower*, 1–50 Hz) bands. Vertical symbols indicate licks. *Bottom*, SWR (*upper*) and lick (*lower*) rates in this session (98 trials).

E, *Left*, Summary of z-scored SWR rate change (*upper*, individual sessions; *lower*, the mean and s.e.m.) around water delivery (0 s) in all sessions (11 sessions from 2 rats). *Right*, Box-and-whisker plots showing decrease in SWR rate after the water delivery (compared between pre and post 1 s windows). Asterisks represent statistical significance by Wilcoxon signed-rank test. $*p < 0.05$, $**p < 0.01$, $***p < 0.001$ in all figures.

F, *Left*, Summary of lick rate in all the sessions. *Right*, Increase in lick rate after the water delivery.

Figure 2 Behavioral performance of False-True Consummation (FTC) task by immobile rats.

A, Pedal hold-release action in response to auditory Go cue for reward water.

B, The FTC task consisting of repetitive pairs of false (unrewarded) and true (rewarded) consummation trials. ITI, intertrial interval; Prep., preparatory action; F./T. cons., false/true consummatory action; RT, reaction time. Gray shaded areas indicate the forbidden range of pedals. Nothing happened for no reward delivery after Correct cue. See **Materials and Methods**.

C, Pedal traces (*upper*, all and median traces) and distribution of the reaction time (*lower*;

arrow indicates median) for false (*gray*) and true (*blue*) consummation trials in a session. We analyzed only correct trials without errors following the previous trials.

D, Lick events in individual trials (*upper*) and lick rate (*lower*), aligned with the onset of Correct cue (*left*) and no (pseudo)-reward/reward delivery (*right*). Horizontal bars indicate time window for anticipatory and intake lick counts.

E, Comparison of averaged reaction time between false and true consummation trials in all sessions (59 sessions from 7 rats). Color circles represent individual rats (filled shows statistical significance for the session). Group analysis showed no significant difference.

F, Comparison of averaged lick rate between false and true consummation trials in all the sessions. Anticipatory (*left*) as well as intake (*right*) lick rates were statistically higher in true consummation trials.

Figure 3 SWR occurrence during FTC task performance.

A, *Top*, SWR events in individual trials (*upper* and *lower*) and SWR rate (*middle*) in false (*gray*) and true (*blue*) consummation trials of a session, aligned with Go cue (*left*; *thick gray*) and pedal release (*right*; *green*), and sorted by the interval. *Bottom*, *upper*, Pedal release rate including the correct reaction and additional pedal releases; *lower*, Lick rate.

B, SWR rate, pedal release rate, and lick rate, aligned with Correct cue (*left*; *thick gray*) and no (pseudo)-reward/reward delivery (*right*; *green*).

C, *Top*, Summary of z-scored SWR rate change (*upper*, individual sessions for false and true consummation trials; *lower*, the mean and s.e.m.) aligned with the correct pedal release (*left*) and no-reward/reward delivery (*right*) in all the 59 sessions. Color circles indicate rats in **Fig. 2*E***. Horizontal bars indicate pre- and post-event time window (1 s) for SWR counts before and after the release (*left*) and no-reward/reward (*right*). *Bottom*, Comparison of SWR rate among the pre and post events in false and true consummation trials. Horizontal lines represent statistical significance (Kruskal Wallis test with post hoc Dunn test).

D, Task events related to the decrease (offset) in SWR rate, as determined by the Phase-Scaling (PS) analysis (Kawabata et al., 2020). *Top*, Onset-to-offset time-course of the SWR occurrence, temporally normalized by the interevent interval (*) between Go cue and release (*left*) and between Correct cue and reward (*right*). Red edge indicates the offset. Note, however, that the SWR offset detection included the subsequent offsets (*left*, after release) and the preceding ones (*right*, before reward), reflecting the two-step nature of the

SWR decreases. *Bottom*, Phase distribution for the offset in the PS analysis. The Phase indicates temporally most related phase to the activity offset. Note that the Phase for offset (i.e., SWR falling) was located between the Go cue and release (*left*) and just after the reward (*right*).

E, Task events related to the SWR offset around the reward. It was much more related to the reward delivery itself than the first lick (*left*) and the first pedal release (*right*) following the reward delivery.

F, Z-scored SWR rate (true consummation trials in all the sessions) aligned with the last lick for reward intake (*left*) and the start of pedal hold for the next trial (*right*).

Figure 4 Spike activity of hippocampal neurons during FTC task performance.

A, Classification of all isolated neurons into regular spiking (RS; *blue*) and fast spiking (FS; *red*) neurons by the spike waveform (trough-to-peak length). The ongoing spike rate (in logarithmic scale; average over the entire recording time) was statistically lower in the RS neurons than the FS neurons.

B, *Left*, Criteria that define task-related neurons (see **Materials and Methods**). Each dot represents task-related (TR; *black*) or non-task-related (NTR; *gray*) neurons. *Right*, Peri-event time histograms (PETHs) of spike activity in representative TR and NTR neurons (a–c).

C, Summary of z-scored spike rate change for four clusters (Clu.1–4) of all TR (RS and FS) neurons, aligned with Go cue and reward of true consummation trials, and Go cue and no reward of false consummation trials (from left to right). Neurons were sorted by the spike peak in the second alignment (true, reward).

D, Spike rate change and task event relevance for the four neuron clusters. *Each top*, Z-scored spike rate change (the mean and s.e.m.), aligned with the Go cue (*left*) and reward (*right*). *Each middle*, Onset-to-offset time-course of the spike activity, temporally normalized (*) by the interval between Go cue and release (*left*) and the Correct cue and reward (*right*). *Each bottom*, Phase distribution in the PS analysis for the offset (Clu.1,2) and onset (Clu.3,4).

Figure 5 Modulation of neural activity by reward expectation and acquisition.

A, Comparison of spike rate (in logarithmic scale) between pre- and post-event time windows (*upper*, Go cue; *lower*, Reward; 1 s) and also between false and true consummation

trials in individual neuron clusters (1–4). Horizontal lines represent statistical significance.
B, Reward modulation indices (RMIs) in the pre Go cue (*abscissa*) and post reward (*ordinate*) time windows. Each symbol represents single neuron (*triangle*, RS; *circle*, FS) colored by its cluster (also including NTR in gray). Black diamond represents SWRs in each session. Large symbols indicate their median. The RMI denotes higher (towards +1) or lower (−1) activity depending on reward expectation (pre Go cue) and acquisition (post reward). Note the SWRs (*black*) overlap with protrusive clu.1 (*green*) and 2 (*blue*) neurons.

Figure 6 Spiking activity in synchrony with SWRs during FTC task performance.
A, Z-scored cross-correlogram (CCG) of spikes to the peak of SWRs (0 s) in individual neurons (all RS and FS neurons).
B, Proportion of spike increase (Inc.; significant in yellow, not significant in light gray) and decrease (Dec.; significant in dark purple, not significant in dark gray) during SWRs in all RS and FS neurons. RS neurons showed significantly more SWR synchrony than FS neurons. Neuron counts and percentages are shown in each pie chart.
C, Proportion of spike increase and decrease during SWRs (with and without statistical significance) in all TR and NTR neurons. TR neurons showed more SWR synchrony than NTR neurons.
D, *Top*, Peak/trough latency of spike increase/decrease from the SRW peak time (0 s). *Bottom*, Distribution of the most active phases of ripple oscillation in the RS (*blue*) and FS (*red*) neurons.
E, Proportion of spike increase and decrease during SWRs in the Clu.1–4 neurons and NTR neurons. The majority of Clu.1–3 neurons exhibited spike increase synchronous with SWRs, but less in Clu.4 and NTR, as shown in the color matrix of statistical effect sizes for all pairs of clusters (*bottom*).
F, Plots of the spike rate (in logarithmic scale) during SWRs (*upper*; ±50 ms from the SWR peak) and ongoing spike rate (*lower*) against the RMI in post reward (*left*), similarity (correlation coefficient *r*) between SWR and spike rate changes around the Go cue (*middle*) and reward (*right*) along the course of true consummation trials. Each dot represents a single neuron colored by cluster (Clu.1–4 and NTR), with a regression line for all dots (*black*). Large dots and bars indicate the median and median absolute value (M.A.D.). Colored asterisks show that the neuron cluster deviated significantly upper or lower from the

regression line (sign test).

G, Cumulative distributions of the spike rate during SWRs (*upper*) and ongoing spike rate (*lower*) shown in ***F***. *Insets*, color of effect size matrices for all cluster pairs.

H, *Left*, Plots of the spike rate during SWRs between false and true consummation trials. Inset shows shifts toward higher peak index in true consummation trials.

Right, Plots of the spike rate during SWRs between off-task (outside task engagement) and on-task (during it) periods. Inset shows shifts toward higher peak index in on-task period.

I, A schematic diagram of hippocampal SWR and spike activity patterns. It shows SWR and spike rate changes along an action-outcome trial (*traces*), and an SWR occurrence with spike increases (*box*). Thick arrows represent possible replay and preplay on Clu.3 signals. See also our hypothesis in the **Discussion**.

Figure 1

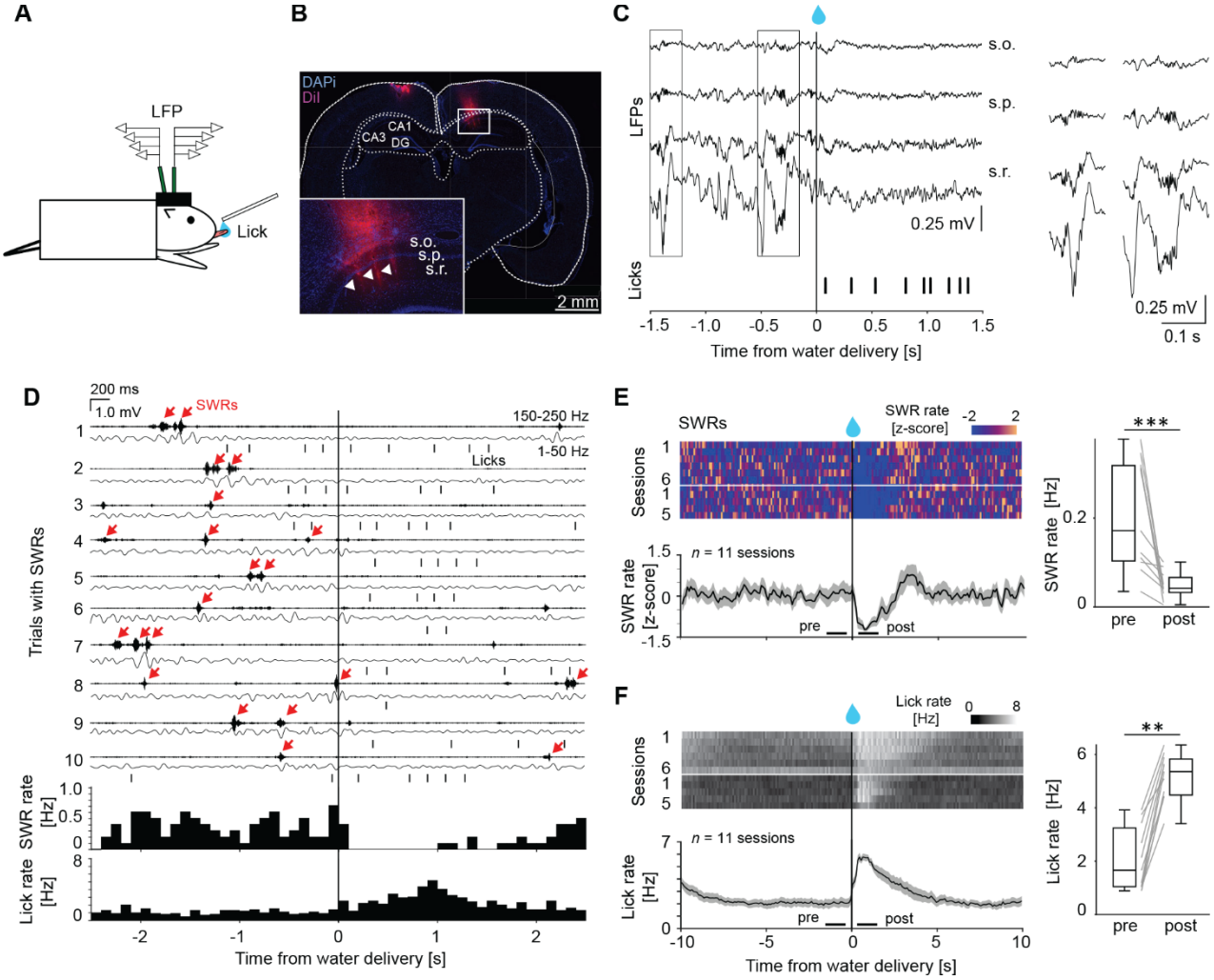
A
LFP
Lick
B
DAPi
DiI
CA1
CA3
DG
s.o.
s.p.
s.r.
2 mm
C
LFPs
s.o.
s.p.
s.r.
0.25 mV
Licks
-1.5
-1.0
-0.5
0
0.5
1.0
1.5
Time from water delivery [s]
0.25 mV
0.1 s
D
200 ms
1.0 mV
SWRs
150-250 Hz
1-50 Hz
Licks
Trials with SWRs
SWR rate [Hz]
Lick rate [Hz]
Time from water delivery [s]
E
SWRs
SWR rate [z-score]
-2
2
Sessions
n = 11 sessions
SWR rate [z-score]
pre
post
***
SWR rate [Hz]
F
Lick rate [Hz]
0
8
Sessions
n = 11 sessions
Lick rate [Hz]
pre
post
Time from water delivery [s]
**
Lick rate [Hz]

Figure 2

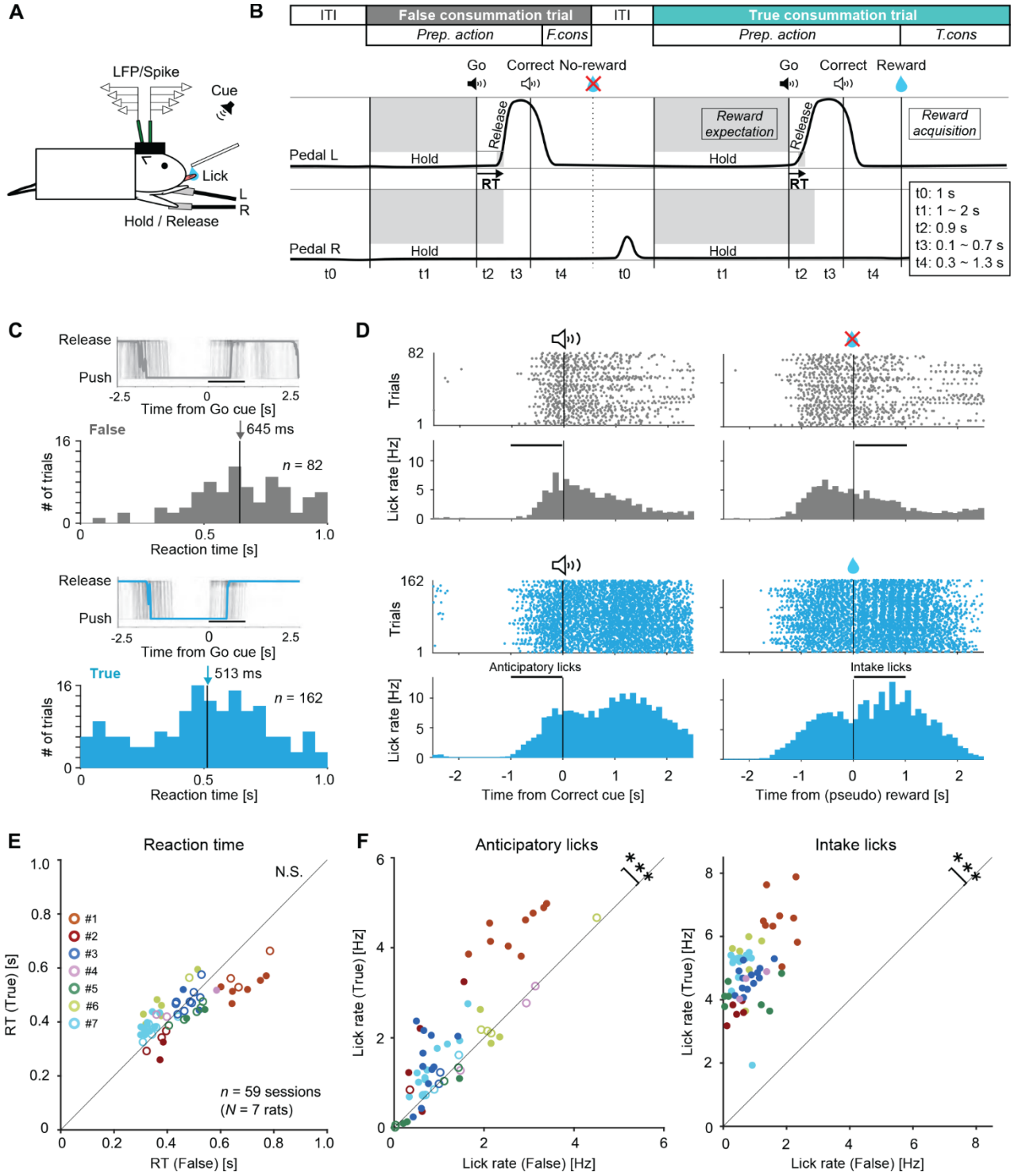
A
LFP/Spike
Cue
Lick
L
R
Hold / Release
B
ITI
False consummation trial
ITI
True consummation trial
Prep. action
F.cons
Prep. action
T.cons
Go
Correct
No-reward
Go
Correct
Reward
Release
Reward expectation
Release
Reward acquisition
Pedal L
Hold
Hold
RT
RT
Pedal R
Hold
Hold
t0: 1 s
t1: 1 ~ 2 s
t2: 0.9 s
t3: 0.1 ~ 0.7 s
t4: 0.3 ~ 1.3 s
t0
t1
t2
t3
t4
t0
t1
t2
t3
t4
C
Release
Push
-2.5
0
2.5
Time from Go cue [s]
False
645 ms
n = 82
# of trials
16
0
0
0.5
1.0
Reaction time [s]
Release
Push
-2.5
0
2.5
Time from Go cue [s]
True
513 ms
n = 162
# of trials
16
0
0
0.5
1.0
Reaction time [s]
D
Trials
82
1
Lick rate [Hz]
10
5
0
Trials
162
1
Anticipatory licks
Intake licks
Lick rate [Hz]
10
5
0
-2
-1
0
1
2
Time from Correct cue [s]
-2
-1
0
1
2
Time from (pseudo) reward [s]
E
Reaction time
N.S.
#1
#2
#3
#4
#5
#6
#7
n = 59 sessions
(N = 7 rats)
RT (True) [s]
1.0
0.8
0.6
0.4
0.2
0
0
0.2
0.4
0.6
0.8
1.0
RT (False) [s]
F
Anticipatory licks
***
Lick rate (True) [Hz]
6
4
2
0
0
2
4
6
Lick rate (False) [Hz]
Intake licks
***
Lick rate (True) [Hz]
8
6
4
2
0
0
2
4
6
8
Lick rate (False) [Hz]

Figure 3

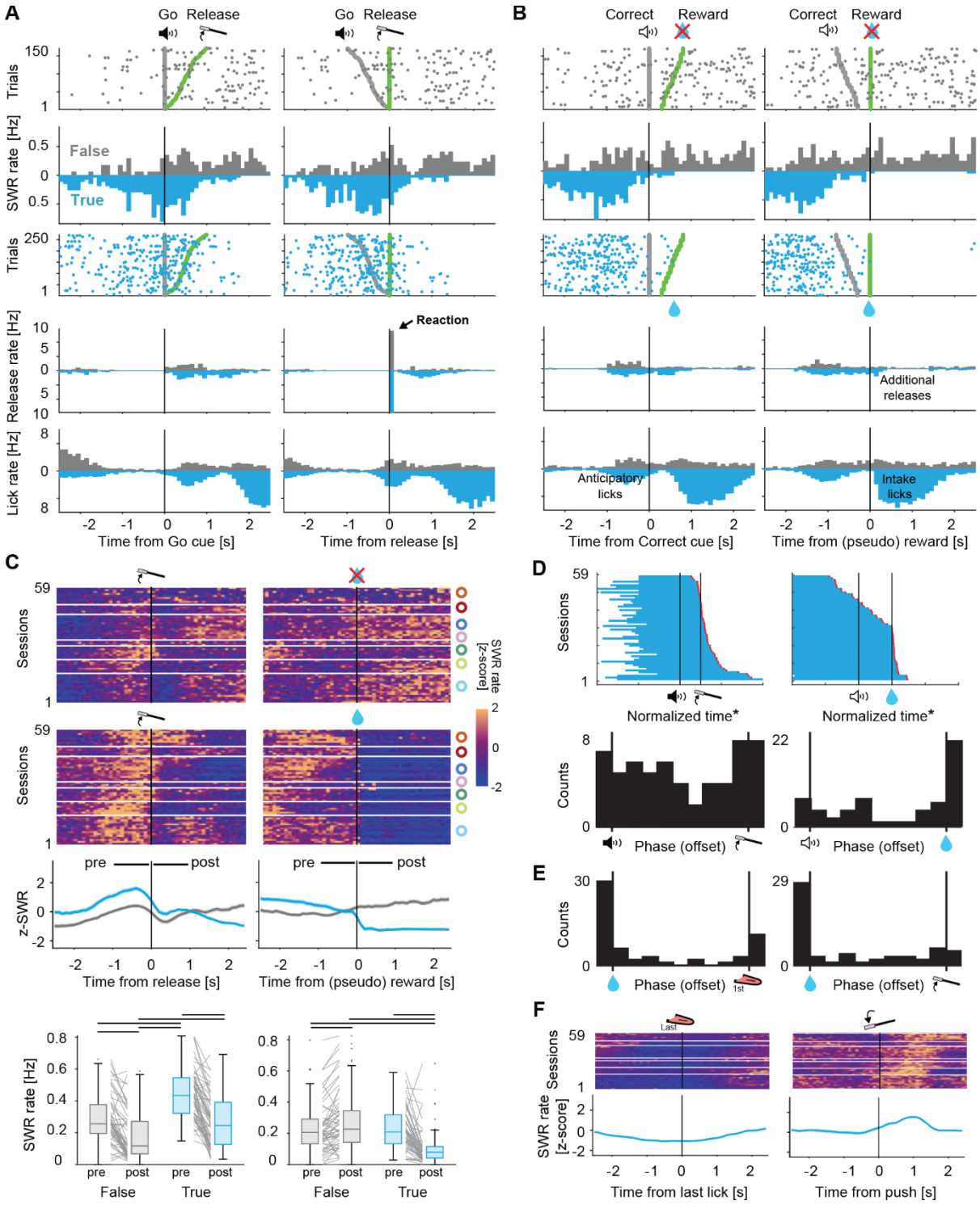
A
Go Release
Go Release
Trials
SWR rate [Hz]
False
True
Reaction
Release rate [Hz]
Lick rate [Hz]
Time from Go cue [s]
Time from release [s]
B
Correct Reward
Correct Reward
Additional releases
Anticipatory licks
Intake licks
Time from Correct cue [s]
Time from (pseudo) reward [s]
C
Sessions
SWR rate [z-score]
pre
post
z-SWR
Time from release [s]
Time from (pseudo) reward [s]
SWR rate [Hz]
False
True
D
Normalized time*
Counts
Phase (offset)
E
1st
F
Last
Time from last lick [s]
Time from push [s]

Figure 4

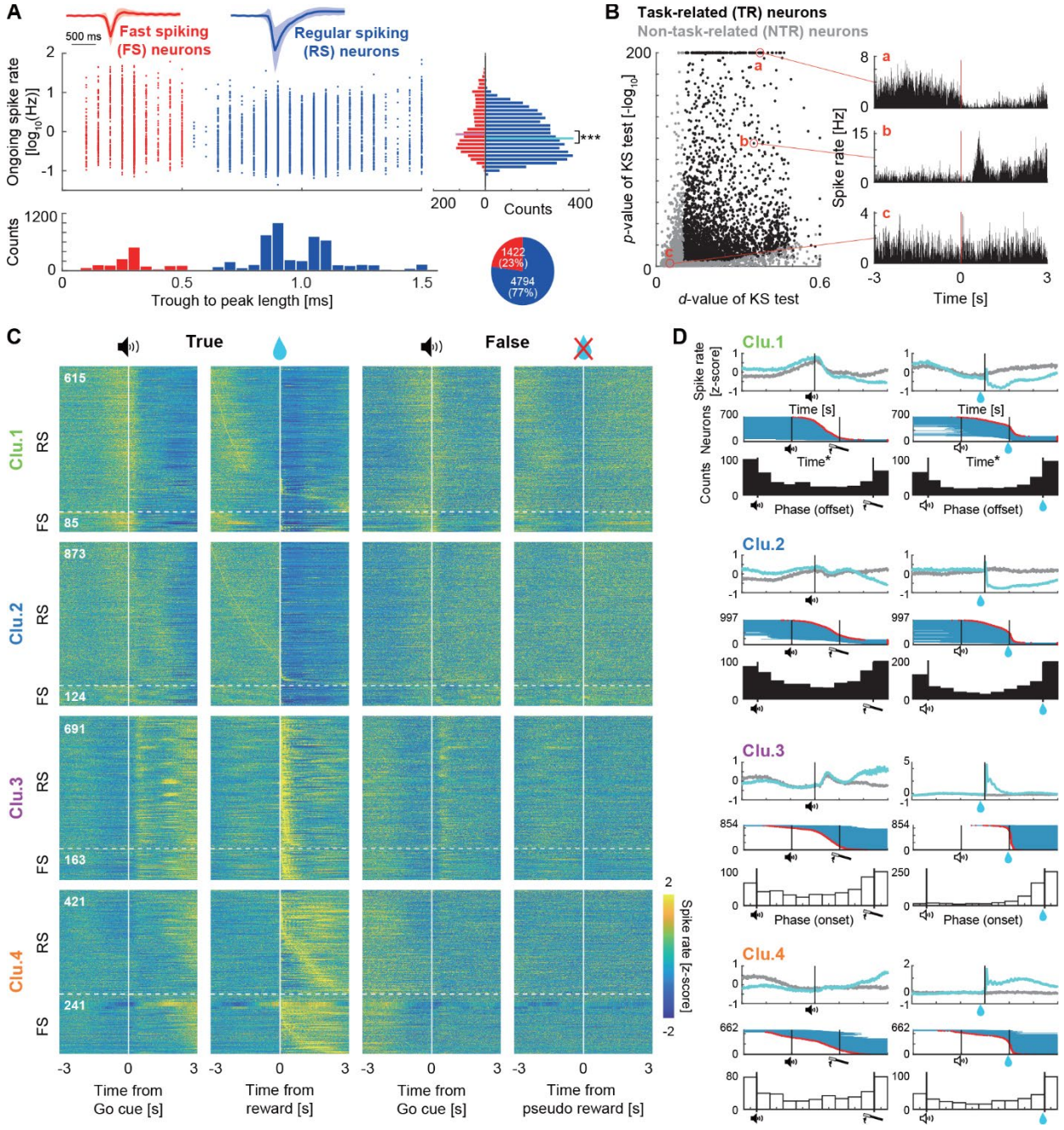
A
500 ms
Fast spiking (FS) neurons
Regular spiking (RS) neurons
Ongoing spike rate [log10(Hz)]
Counts
Trough to peak length [ms]
***
1422 (23%)
4794 (77%)
B
Task-related (TR) neurons
Non-task-related (NTR) neurons
p-value of KS test [-log10]
d-value of KS test
Spike rate [Hz]
Time [s]
C
True
False
Clu.1
Clu.2
Clu.3
Clu.4
RS
FS
Time from Go cue [s]
Time from reward [s]
Time from pseudo reward [s]
Spike rate [z-score]
D
Spike rate [z-score]
Neurons
Counts
Time [s]
Time*
Phase (offset)
Phase (onset)

Figure 5

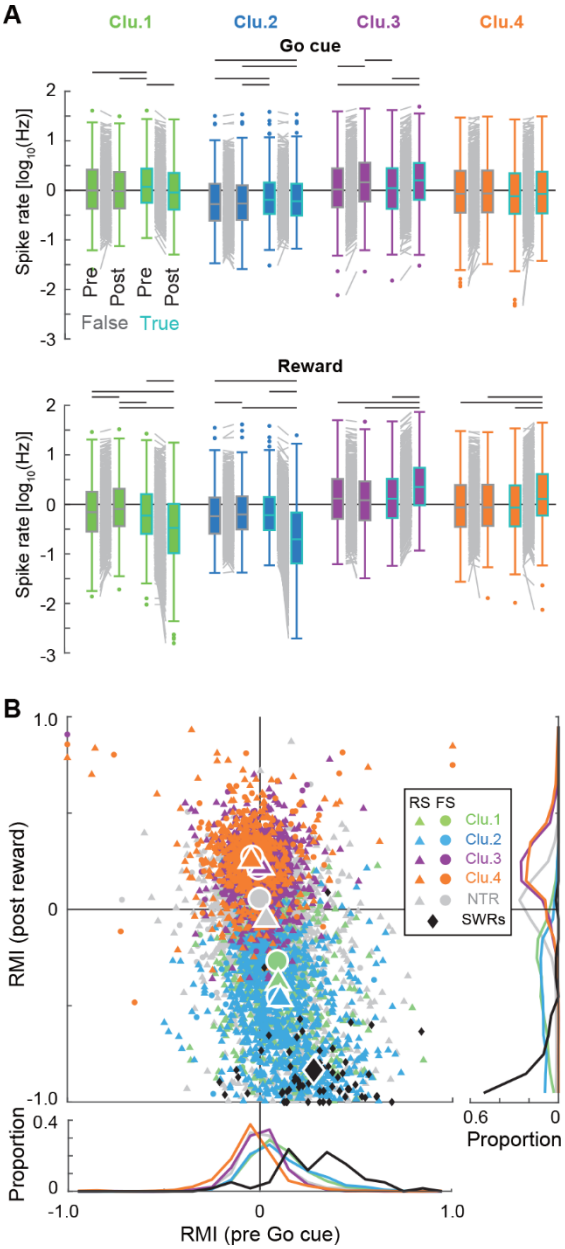
A
Clu.1
Clu.2
Clu.3
Clu.4
Go cue
Spike rate [log10(Hz)]
Pre
Post
Pre
Post
False
True
Reward
B
RMI (post reward)
RS FS
Clu.1
Clu.2
Clu.3
Clu.4
NTR
SWRs
Proportion
RMI (pre Go cue)

Figure 6

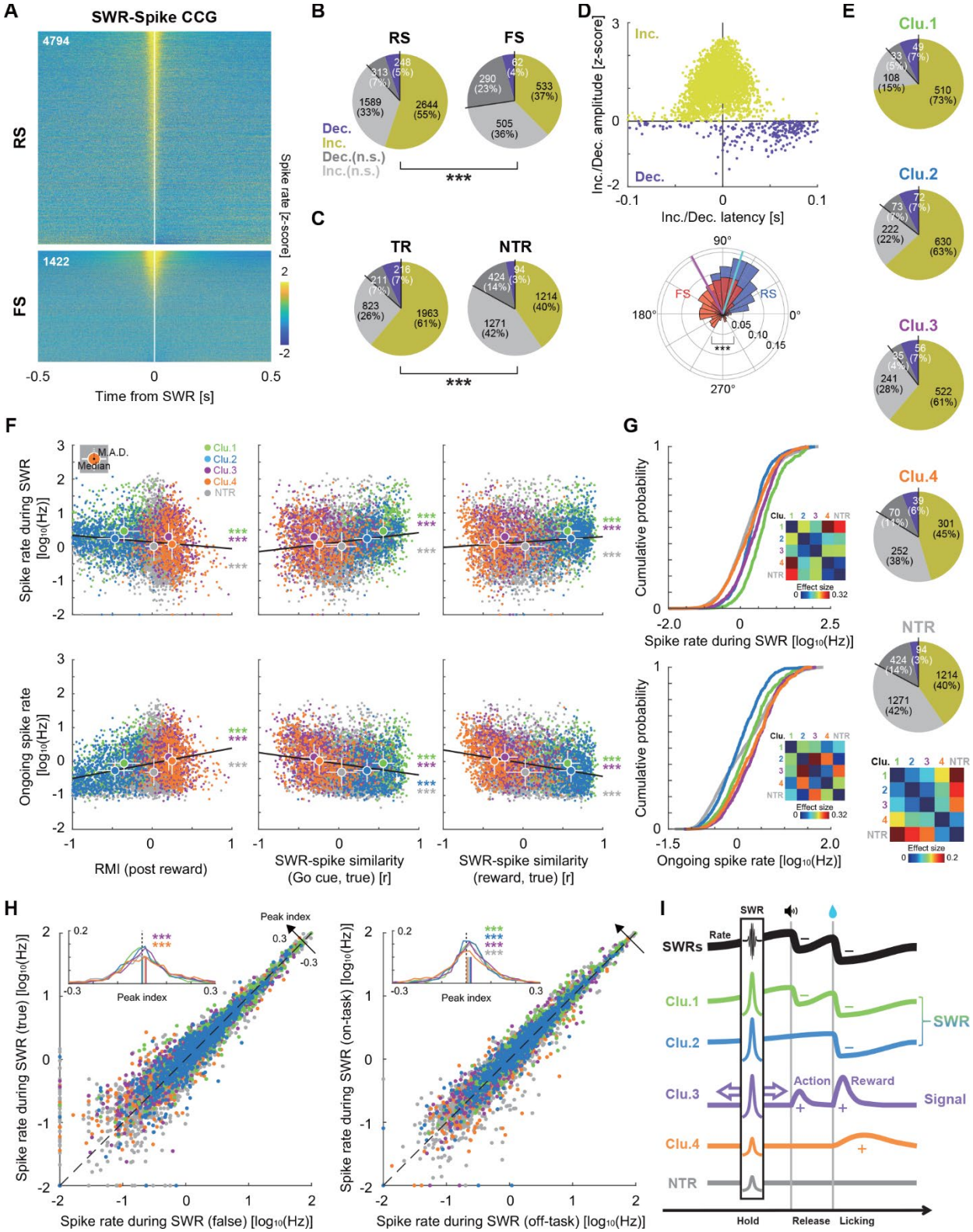
A
SWR-Spike CCG
4794
1422
RS
FS
Spike rate [z-score]
Time from SWR [s]
B
RS
FS
Dec.
Inc.
Dec.(n.s.)
Inc.(n.s.)
C
TR
NTR
D
Inc./Dec. amplitude [z-score]
Inc./Dec. latency [s]
E
Clu.1
Clu.2
Clu.3
Clu.4
NTR
F
M.A.D.
Median
Clu.1
Clu.2
Clu.3
Clu.4
NTR
Spike rate during SWR [log10(Hz)]
Ongoing spike rate [log10(Hz)]
RMI (post reward)
SWR-spike similarity (Go cue, true) [r]
SWR-spike similarity (reward, true) [r]
G
Cumulative probability
Spike rate during SWR [log10(Hz)]
Ongoing spike rate [log10(Hz)]
Effect size
H
Peak index
Spike rate during SWR (true) [log10(Hz)]
Spike rate during SWR (false) [log10(Hz)]
Spike rate during SWR (on-task) [log10(Hz)]
Spike rate during SWR (off-task) [log10(Hz)]
I
SWR
Rate
SWRs
Clu.1
Clu.2
Clu.3
Clu.4
NTR
Action
Reward
Signal
Hold
Release
Licking